ELSEVIER

Journal of Chromatography A, 973 (2002) 97–101

JOURNAL OF CHROMATOGRAPHY A

www.elsevier.com/locate/chroma

Size-exclusion chromatography of low-molecular-mass polymers using mesoporous silica

Terry Nassivera, Andrew G. Eklund, Christopher C. Landry*

Department of Chemistry, University of Vermont, Cook Physical Sciences Building, Burlington, VT 05405, USA

Received 24 September 2001; received in revised form 5 August 2002; accepted 6 August 2002

Abstract

In this study, the mesoporous silicas APMS-30 and MCM-41 were compared to a commercial silica, Nucleosil, in size-exclusion chromatography (SEC). Polystyrenes of various molecular masses (M) were passed through HPLC columns of the silicas (each column contained a single type of silica) and retention times were plotted as a function of log M for each type of silica. Linear fits to the data were used to identify regions of total exclusion, size exclusion, and total permeation in each of the three plots. Due to their small pore sizes, APMS-30 and MCM-41 (pore radii: 14.5 and 17.0 Å from N_2 physisorption, respectively) did not exhibit a total permeation region even at $M=104$ g mol^{-1} (styrene monomer), while Nucleosil (pore radius: 57.9 Å) showed total permeation at $M=644$ g mol^{-1}. These results indicate that mesoporous silica is better than Nucleosil in SEC of polymers with low M, making it useful in a variety of SEC applications including the determination of M for small molecules such as oligomers and oligopeptides. Interestingly, calculation of the radius of gyration, R_g, of the largest polymer that still exhibits a size-exclusion effect proved to be a reasonable method of determining the pore diameters of each material, with estimated $R_g=8.9$, 11.5, and 63.5 Å for APMS-30, MCM-41, and Nucleosil, respectively.

Keywords: Stationary phases, LC; Low-molecular-mass polymers; Mesoporous silica; Polystyrene

1. Introduction

Size-exclusion chromatography (SEC), also known as gel permeation chromatography, is a technique commonly used to determine molecular masses and distributions of polymers and oligopeptides [1–4]. In these applications, an organic polymer is commonly used as the solid phase through which the separations are performed. However, problems with degradation of organic polymers can make them undesirable as solid phases; in addition, they must be swelled in an appropriate solvent prior to use and are sensitive to solvent conditions. For example, polystyrene columns must be used with organic solvents as the mobile phase; exposure to water can cause irreversible column damage.

Porous silica can also be used as the solid phase in SEC. It has the advantage of being rigid, which is beneficial for high pressure separations, and is also easily modified for use in separating a variety of molecules. Silica can also be used with a much wider variety of mobile phases than polymer-based stationary phases. Recently, a type of silica was developed

*Corresponding author. Fax: +1-802-656-8705.
E-mail address: cclandry@zoo.uvm.edu (C.C. Landry).

0021-9673/02/$ – see front matter
PII: S0021-9673(02)01200-1

that is mesoporous, with a typically narrow pore size distribution, and can be synthesized with a particle morphology of monodisperse spheres 4–10 μm in diameter. This material, APMS-30 (acid-prepared mesoporous spheres, pore diameter: 30 Å) [5] has a surface area three to four times that of commercially available chromatographic grade silica and produces analyte retention factors (k') approximately four times larger than commercial silica. APMS-30 is also easily modified for use in reversed-phase and chiral separations, with similar increases in retention factors over commercially available silica [6]. In this report, the results of the use of APMS-30 in SEC are presented. The performance of this material is compared to another mesoporous silica, MCM-41 [7–9]. Although MCM-41 and APMS-30 have approximately the same surface area, pores are much more ordered in the former material and the particle morphology is highly irregular and variable in size.

2. Experimental

2.1. Materials

APMS-30 and MCM-41 were prepared as previously described [5,6,8–11]. Nucleosil-50 was obtained from Phenomenex. Polystyrenes were purchased from Aldrich (MW: 679 000; 29 300; 13 700; 3680; 2430; 760; and 104.15 g mol^{-1}) and Polysciences (MW: 980; 517; and 345 g mol^{-1}) and used as received. HPLC-grade THF was obtained from J.T. Baker and used as received. A Hewlett-Packard (Boston, MA, USA) Series 1100 HPLC was used for these experiments. Columns were packed using a Shandon (Astmoor, Cheshire, UK) column packer. Powder X-ray diffraction (XRD) experiments were performed on a Scintag X1 θ-θ diffractometer equipped with a Peltier (solid-state thermoelectrically cooled) detector using Cu Kα radiation. Nitrogen adsorption and desorption isotherms were obtained on a Micromeritics ASAP 2010 instrument. Samples were degassed at 200 °C under vacuum overnight prior to measurement. Surface areas were measured using the BET method and pore size distributions were calculated using the modified BJH method developed by Kruk, Jaroniec and Sayari [12–14].

2.2. Methods

To perform the SEC experiments, two 4.6×200 mm stainless steel high pressure liquid chromatography (HPLC) columns (O.D. 0.25 in) were slurry packed with 4.0–6.0 g of silica in THF under 1.4 bar of N_2. The columns were then joined by a 35 mm stainless steel connector and connected as a unit to the HPLC instrument. Approximately 9 mg of polymer was then dissolved in 2 ml THF, and 5 μl of this solution was injected onto the column via a manual injector. THF was also used as the mobile phase. The pressure on the columns was 40 bar for mesoporous silica and 70 bar for commercial silica, and the flow-rate was 1.00 ml min^{-1}. Detection of the polymer was performed at 254 nm. A minimum of three trials for each polystyrene (PS) were used to obtain the data.

3. Results and discussion

A calibration curve for 50 Å-Nucleosil, a silica with the smallest commercially available pore diameter, is shown in Fig. 1. Linear fits are shown for the total permeation, size exclusion, and total exclusion regions of the graph. Of the three, only the size

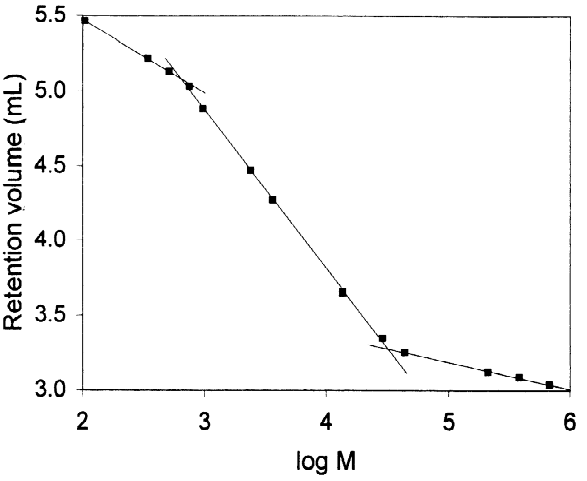

Fig. 1. Calibration curve for the separation of PS using Nucleosil as the solid support. Molecular masses of PS, in g mol^{-1}: 104 (monomer), 345, 517, 760, 980, 2430, 3680, 13 700, 29 300, and 679 000.

exclusion region can be used to determine molecular masses, since different retention times for PS in this region are based mainly on entropic considerations related to the size of the pores of the stationary phase [1–3]. SEC operates under conditions where molecules partition between the volumes on the interior and exterior of the stationary phase. Any differential retention in the total permeation and total retention regions of the plot is due mainly to enthalpic interactions with the silica.

The intersection of the lines drawn through the size exclusion and total exclusion regions of the Nucleosil calibration can be used to determine M for the largest PS that still fit inside the pores of the silica. This ''molecular mass cut-off'' is therefore a measure of the largest polymer that still exhibits mainly entropic interactions with the silica. For Nucleosil, this cut-off corresponds to $M=32\,600$ g mol^{-1}. Assuming a hard-sphere model for the PS and cylindrical pores for Nucleosil, the approximation:

$$R_g(\text{Å}) = 0.137M^{0.589}$$

can be used to relate the molecular mass of the PS to its radius of gyration (R_g), which is its effective radius in solution [1–3]. R_g at the molecular mass cut-off should therefore be approximately equal to the pore radius of the substrate (Table 1). For the value of M given above, $R_g=63.5$ Å, which is in contrast to the stated average pore radius for Nucleosil of 25 Å. However, N_2 physisorption experiments (Table 1) confirmed that the average pore radius was actually 57.9 Å. The difference between the values obtained by the two methods is likely related to the wide distribution in pore radii for Nucleosil. Similar calculations at the intersection of the lines drawn through the size exclusion and total *permeation* regions give information about the smallest polymer that still shows a size exclusion effect. This calculation gives $M=644$ g mol^{-1} and $R_g=6.2$ Å. This stationary phase therefore is ineffective for small PS oligomers.

The results for Nucleosil are in contrast to the data obtained for APMS-30 and MCM-41 (Fig. 2), which do not exhibit a total permeation region. Size exclusion effects are observed even for the styrene monomer ($M=104$ g mol^{-1}) for both types of silica. N_2 physisorption data for these materials show much smaller pore radii and the molecular mass cut-offs for these materials are correspondingly small ($M=$ 1210 and 1840 g mol^{-1}, respectively), leading to values of $R_g=8.9$ and 11.5 Å. This data and the result for Nucleosil shown above confirm the usefulness of SEC in predicting the pore radius of the stationary phase. It is also interesting to note the relative accuracy of the stationary phases in determining M for each polymer (Table 2). Nucleosil, MCM-41 and APMS-30 all have average errors of 3–4% in M. It should be noted that the mesoporous silicas show less absolute error in M than Nucleosil over their respective size exclusion ranges. For example, APMS-30 gave a 1.82% error for $M=104$

Table 1
Physical data for the silicas used in this study

	Nucleosil	APMS-30	MCM-41
Surface area ($m^2\,g^{-1}$)	369	1130	1260
Pore volume ($cm^3\,g^{-1}$)	0.837	0.647	1.02
Total porosity (%)[a]	75	73	82
Average pore diameter (Å)	116	29.2	33.8
PWHM of PSD (Å)[b]	107	11.2	4.84
Particle size (μm)[c]	4–6	4–10	1–50

[a] Calculated using retention time of styrene monomer.
[b] Peak width at half maximum of the pore size distribution.
[c] Determined by electron microscopy.

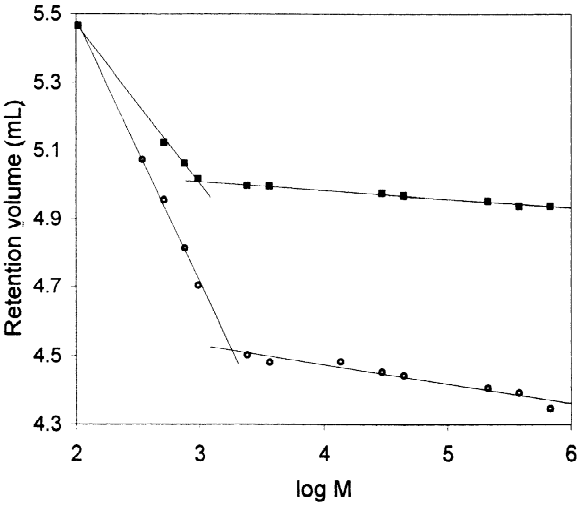

Fig. 2. Calibration curve for the separation of PS using APMS-30 (squares) and MCM-41 (circles) as the solid support. PS molecular masses are the same as those given in Fig. 1.

Table 2
Over- or under-estimation of M for PS in the size exclusion region

Given MW ("f_0", g mol^{-1})	Nucleosil			MCM-41			APMS-30		
	Est. MW from plot ("f", g mol^{-1})	f/f_0	Over/under-estimation (%)	Est. MW from plot ("f", g mol^{-1})	f/f_0	Over/under-estimation (%)	Est. MW from plot ("f", g mol^{-1})	f/f_0	Over/under-estimation (%)
29 300	27 900	0.952	4.84						
13 700	14 400	1.05	4.84						
3680	3770	1.02	2.33						
2430	2440	1.00	0.402						
980	1000	1.02	2.12	1040	1.06	5.92	943	0.962	3.82
760	727	0.957	4.36	748	0.985	1.54	751	0.989	1.14
517				488	0.944	5.56	553	1.07	6.95
345				343	0.995	0.491			
104				106	1.02	2.22	102	0.982	1.82
Avg.			3.15			3.15			3.43

g mol^{-1}, an absolute error of 2 g mol^{-1}. The same % error for $M=3680$, in the center of the size exclusion range for Nucleosil, would lead to an absolute error of 67 g mol^{-1}. The performance of the mesoporous silica is impressive for this reason, but also due to its ability to perform SEC even at extremely small values of M. This ability to separate very small molecules may lead to new applications in SEC in molecular mass determinations of short oligomers and oligopeptides that were previously inaccessible by this method.

It is important to consider the meaning of the molecular mass cut-off for each type of silica. The broad distribution of pore radii for Nucleosil is useful for molecular mass calibrations of PS with low to medium M, since it extends the useful SEC range of this substrate. However, this distribution also has the effect of blurring the molecular mass cut-off points, since the total number of pores with a particular size controls how many polymers are separated by entropic rather than enthalpic considerations. In recognition of this fact, calibration curves such as Fig. 1 are often fitted with an exponential curve rather than a series of lines. In contrast, the substantially more narrow distributions of pore radii for APMS-30 and MCM-41 may perhaps limit their useful ranges, but the molecular mass cut-offs for these materials are more significant and the calibration data may be more appropriately used with linear rather than exponential fitting.

Average peak widths for the various regions of each calibration curve are given in Table 3. In general, the mesoporous silicas show broader peaks than Nucleosil. This is expected due to the larger surface areas of the mesoporous materials, since this may increase any adsorption effects due to interactions of the PS with the silica surface. Previous studies concluded that this adsorption effect did not substantially influence the ability of silica (as opposed to a polymer-based substrate) to serve as a substrate for SEC, since reversed-phase silica showed a similar adsorption effect [15]. Of the two mesoporous silicas, APMS-30 shows unusually broad peaks. The major differences between the two

Table 3
Curve-fitting and peak width information for the plots in Figs. 1 and 2

	Nucleosil				MCM-41				APMS-30			
	Slope (ml)	Intercept (ml)	Avg. peak width (ml)	R^2	Slope (ml)	Intercept (ml)	Avg. peak width (ml)	R^2	Slope (ml)	Intercept (ml)	Avg. peak width (ml)	R^2
Total permeation	−0.479	6.431	0.1953	0.999								
Size exclusion	−1.06	8.072	0.2166	0.999	−0.769	7.024	0.4783	0.998	−0.465	6.399	1.213	0.998
Total exclusion	−0.181	4.091	0.0790	0.997	−0.057	4.700	0.3375	0.933	−0.025	5.081	1.172	0.983

materials are the particle shape, distribution of particle diameters, and pore ordering. Since the first property is expected to have the opposite effect on peak width and the second should have little if any effect, one may speculate that the difference in pore structure is the source of the peak broadening. However, further experiments are required to confirm this point more definitively.

Acknowledgements

This work was supported by the University of Vermont, by the NSF CAREER program (CHE-9875768), and by the NSF EPSCoR program under Cooperative Agreement EPS-9874685.

References

[1] S. Mori, H.G. Barth, Size Exclusion Chromatography, Springer, Berlin, 1999.
[2] W.W. Yau, J.J. Kirkland, D.D. Bly, Modern Size Exclusion Chromatography, Wiley, New York, 1979.
[3] B.J. Hunt, S.R. Holding, Size Exclusion Chromatography, Blackie, Glasgow, 1989.
[4] H.G. Barth, B.E. Boyes, C. Jackson, Anal. Chem. 70 (1998) 251R.
[5] K.W. Gallis, J.T. Araujo, K.J. Duff, J.G. Moore, C.C. Landry, Adv. Mater. 11 (1999) 1452.
[6] K.W. Gallis, A.G. Eklund, S.T. Jull, J.T. Araujo, J.G. Moore, C.C. Landry, Stud. Surf. Sci. Catal. 129 (2000) 747.
[7] C.T. Kresge, M.E. Leonowicz, W.J. Roth, J.C. Vartuli, J.S. Beck, Nature 359 (1992) 710.
[8] J.S. Beck, J.C. Vartuli, W.J. Roth, M.E. Leonowicz, C.T. Kresge, K.D. Schmitt, C.T.-W. Chu, D.H. Olson, E.W. Sheppard, S.B. McCullen, J.B. Higgins, J.L. Schlenker, J. Am. Chem. Soc. 114 (1992) 10834.
[9] K.W. Gallis, C.C. Landry, Chem. Mater. 9 (1997) 2035.
[10] C.C. Landry, S.H. Tolbert, K.W. Gallis, A. Monnier, G.D. Stucky, P. Norby, J.C. Hanson, Chem. Mater. 13 (2001) 1600.
[11] S.H. Tolbert, C.C. Landry, G.D. Stucky, B.F. Chmelka, P. Norby, J.C. Hanson, Chem. Mater. 13 (2001) 2247.
[12] M. Kruk, V. Antochshuk, M. Jaroniec, A. Sayari, J. Phys. Chem. B 103 (1999) 10670.
[13] M. Kruk, M. Jaroniec, Y. Sakamoto, O. Terasaki, R. Ryoo, C.-H. Ko, J. Phys. Chem. B 104 (2000) 292.
[14] M. Kruk, M. Jaroniec, A. Sayari, Langmuir 13 (1997) 6267.
[15] D.M. Northrop, R.P.W. Scott, D.E. Martire, Anal. Chem. 63 (1991) 1350.